Metrology For High-Frequency Nanoelectronics*

T. Mitch Wallis, Atif Imtiaz, Hans T. Nembach, Paul Rice, and Pavel Kabos

National Institute of Standards and Technology, 325 Broadway, Boulder, CO 80305

Abstract. Two metrological tools for high-frequency measurements of nanoscale systems are described: (i) two/N-port analysis of nanoscale devices as well as (ii) near-field scanning microwave microscopy (NSMM) for materials characterization. Calibrated two/N-port measurements were made on multiwalled carbon nanotubes (MWNT) welded to a coplanar waveguide. Significant changes in the extracted high-frequency electrical response of the welded MWNT were measured when the contacts to the MWNT were modified. Additionally, NSMM was used to characterize films of nanotube soot deposited on copper and sapphire substrates. The material properties of the films showed a strong dependence on the substrate material.

Keywords: calibration, carbon nanotubes, microwaves, near-field electromagnetics, radio frequency nanoelectronics, scanning probe microscopy,
PACS: 06.20.fb, 41.20.Jb, 73.63.Fg

INTRODUCTION

The push of the electronics and storage industries toward device sizes at nanometer scale and operating frequencies of 100 GHz and beyond demands a new physical understanding of the electromagnetic properties of nanoscale objects at these frequencies. New metrological tools are required, as existing techniques often do not scale with device size or operating frequency. Below, we discuss two metrological tools for high frequency measurements at nanometer length scales: (i) two/N-port analysis of nanoscale devices as well as (ii) near-field scanning microwave microscopy (NSMM) for materials characterization.

A number of studies have suggested the viability of nanotubes and nanowires for high-frequency applications, including nanotube-based transistors [1-3]. Though a number of studies have measured the high-frequency response of carbon nanotubes [4-7], this metrology is at an early stage of development. Many of these measurements were single-port measurements and do not provide the richer set of information that is available via two-port measurements. In the first half of this paper, we describe how standard calibration and extraction techniques can be applied to two-port measurements of a multiwalled carbon nanotube (MWNT) to extract the high-frequency electrical response of the tube and its contacts. Systematic modification of the contacts leads to measurable changes in the response.

It is highly desirable to supplement the two-port measurements of the high-frequency response of nanoscale systems with complementary, spatially-resolved measurements of the material properties of nanoscale systems. To this end, a number of high-frequency, scanning probe techniques are under development [8-11]. In order to achieve a useful spatial resolution, the sample-probe distance must be on the order of the probe dimension, i.e., in the near field where the distance is much smaller than the wavelength. In the second half of this paper, we describe measurements of thin films of nanotube soot with NSMM. We observe that the underlying substrate has a strong effect on the material properties of the nanotube film.

TWO/N-PORT ANALYSIS OF NANOSCALE SYSTEMS

High-frequency (from 100 MHz to 100 GHz) measurements at the nanoscale present a unique set of challenges, including impedance mismatch, strong frequency dependence of the device impedance, and the need to distinguish the properties of nanoscale devices under test (DUT) from the measurement platform. Additionally, the electronic properties of a nanoscale system such as a nanowire or carbon

nanotube depend sensitively on the nature and quality of the electrical contacts to the system. Here, we combine standard thru-reflect-line (TRL) calibration techniques [12] with an extraction technique [7] to measure the high-frequency response of a MWNT and its contacts. We observe that modifications of the contacts lead to changes in the amplitude and phase of the admittance matrix elements of the device.

Experiment

A schematic of the measurement setup is shown in Figure 1. A single MWNT was welded across a gap in a coplanar waveguide (CPW) structure that served as the DUT. The MWNT was taken from a batch of nanotubes synthesized by chemical vapor deposition on a thin-film Fe catalyst. Xylene and ferrocene were the precursor gases and the furnace temperature during synthesis was 725 °C. The contacts between the MWNT and the CPW were formed in a scanning electron microscope via electron-beam-induced-deposition (EBID) of carbon [13]. The MWNT as originally welded is also shown in Figure 1. Note that the CPW structure was intended for both two- and four-port measurements and includes four leads as well as four ground planes. Only two of the leads were used in the experiments described here. The CPW was contacted by two ground-signal-ground (GSG) probes. The **S** matrix elements (S_{11}, S_{12}, S_{21}, and S_{22}) of the system were measured with a commercial vector network analyzer (VNA). The wafer on which the CPW was patterned also included a set of calibration structures as well as an identical, empty CPW structure. These additional patterned structures were measured with the VNA and were used to perform the calibration and extraction analysis described below.

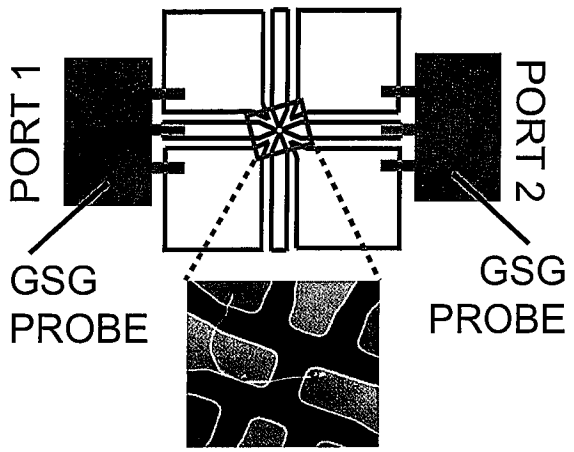

FIGURE 1. Schematic of two-port measurement of a MWNT welded to a CPW. A 20 μm x 15 μm image of the welded MWNT is also shown.

Calibration and Modeling

The measurements of the CPW both empty and with the MWNT were calibrated with the TRL method [12]. This is a standard calibration technique that is well established within the microwave measurement community. The calibration procedure determines the propagation constant of the CPW material. This, in turn, allows the reference planes for the calibrated measurements to be moved up to the edge of the welds of the MWNT. Thus, the electronic properties of the CPW up to the welds are removed from the measurement, providing sensitivity to the high-frequency properties of the MWNT as well as the contacts.

In order to extract the properties of the high-impedance MWNT from the measured data, we used a procedure similar to that developed by Bethoux et. al. [7]. Initially, the measured **S** matrix elements were converted to admittance matrix elements (Y_{11}, Y_{12}, Y_{21}, and Y_{22}). The elements of the Y matrix are algebraic functions of the elements of the **S** matrix parameters [14]. Subsequently, the admittance matrix of the complete welded system ($\mathbf{Y_{total}}$) was modeled as a sum of the admittance matrix of the MWNT and contacts ($\mathbf{Y_{MWNT}}$) and the admittance matrix of the gap ($\mathbf{Y_{gap}}$):

$$Y_{total} = Y_{MWNT} + Y_{gap} \quad . \tag{1}$$

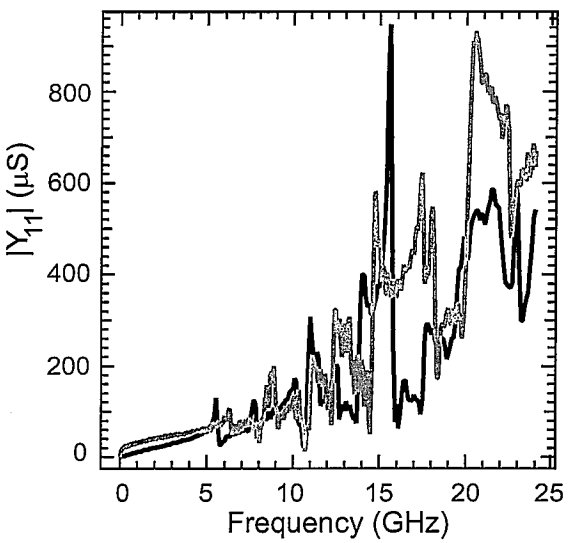

FIGURE 2. Admittance amplitude $|Y_{11}|$ of the MWNT between 10 MHz and 24 GHz: as originally welded (black curve) and with additional carbon added (gray curve).

$\mathbf{Y}_{total}$ and $\mathbf{Y}_{gap}$ are known from the calibrated measurements of the CPW with the MWNT and the empty CPW, respectively. Thus, $\mathbf{Y}_{MWNT}$ can be determined algebraically. For the remainder of the paper, Y_{11}, Y_{12}, Y_{21}, and Y_{22} will refer to the elements of $\mathbf{Y}_{MWNT}$. We will refer to the amplitude of the matrix element Y_{ij} as $|Y_{ij}|$ and the phase in degrees as $\arg(Y_{ij})$.

Results and Discussion

The amplitude $|Y_{11}|$ between 10 MHz and 24 GHz for the MWNT and contacts as originally welded is shown as the black curve in Figure 2. Note that there are a number of sharp peaks in the admittance, particularly above 5 GHz. These peaks were repeatable and are attributed to coupling between different arms of the CPW structure. We modified each of the contacts by adding more carbon to each contact via the EBID process and then repeated the measurements as well as the calibration and extraction analyses. The amplitude $|Y_{11}|$ of the MWNT and modified contacts is shown as the gray curve in Figure 2. Clearly, the modification of the contacts altered the high-frequency electrical response. Note that the difference between the curves can not be accounted for merely by the calibrated measurement uncertainty [15]. Similar modifications were observed in $|Y_{22}|$.

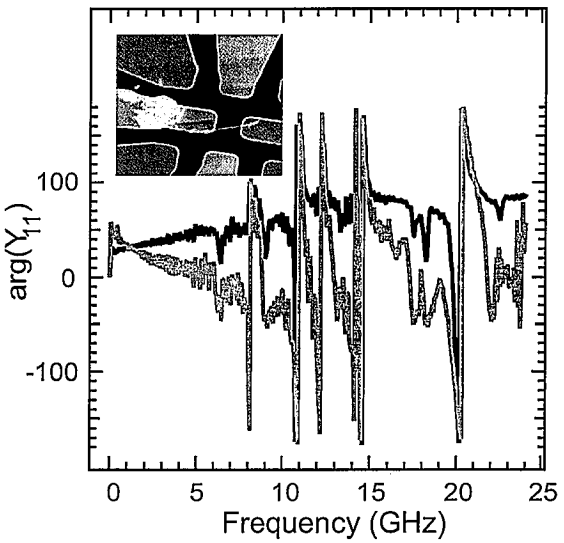

FIGURE 3. Admittance phase $\arg(Y_{11})$ of the MWNT between 10 MHz and 24 GHz before (black curve) and after (gray curve) the removal of the tail. Inset shows welded MWNT without tail.

In addition to the changes observed in the amplitude $|Y_{11}|$, changes in the phase $\arg(Y_{11})$ were also observed upon modification of the contacts. The black curve in Figure 3 shows the phase $\arg(Y_{11})$ between 10 MHz and 24 GHz for the MWNT with modified contacts. Note that $\arg(Y_{11})$ increases, particularly between 10 MHz and 5 GHz. The contact was further modified by removing the "tail" of the MWNT that is visible in Figure 1. The MWNT with the tail removed, shown in the inset to Figure 3, was subsequently measured. The extracted $\arg(Y_{11})$ for the MWNT without the tail is shown as the gray curve in Figure 3. Modification of $\arg(Y_{11})$ is clear. In particular, $\arg(Y_{11})$ now decreases between 10 MHz and 5 GHz.

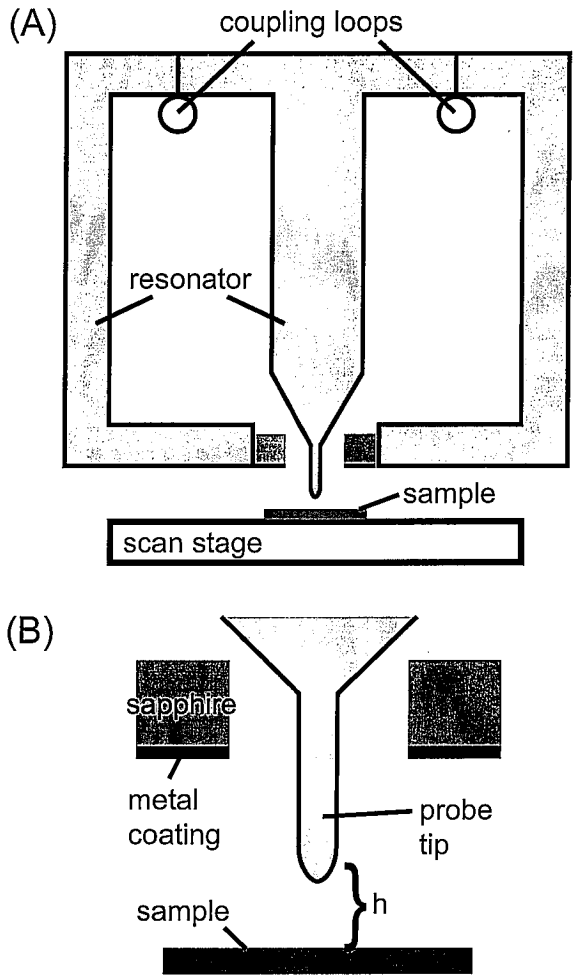

FIGURE 4. A schematic of the NSMM (After reference 8). A wide view of the resonant cavity is shown in (A) and a close-up view of the probe-sample junction is shown in (B).

SCANNING NEAR-FIELD MICROWAVE MICROSCOPY

One of the key motivations driving the development of NSMM is the possibility of measuring high-frequency material properties, such as permittivity. The NSMM used for the measurements described here is based on a needle probe that emerges from the center conductor of a coaxial resonator cavity. As the probe is brought closer to the material sample the quality factor (Q) changes and the resonant frequency (f) shifts. From the dependence of these quantities on probe height above the sample, material properties of the sample may be calculated. However, reliable, quantitative models are still under development. Here, we measure the changes in Q and f for thin films of nanotube soot on bulk copper and sapphire substrates.

Experiment

The NSMM used in these experiments is similar to the one described in Reference 8. A schematic of the NSMM is shown in Figure 4. The sample probe consists of a metal tip that extends from the center conductor of a high-Q, 2.66 GHz coaxial resonator through an aperture at the end of the resonator. The tip has a diameter of about 60 μm and the end of the tip extends about 1.2 mm past the end of the resonator. A two-port VNA is connected to the resonator via each of the two coupling loops. The resonator is mounted on a vertical positioning stage that controls the height of the probe above the sample (h). When the tip is positioned within one millimeter of the sample, evanescent waves from the tip interact with the sample. The sample presents an additional load to the resonator, leading to a change in Q and shift in f. The Q and the shift in resonant frequency (Δf) are determined by measuring the S_{12} parameter with the VNA as a function of frequency and fitting the resonance curve. The sample is mounted on a lateral scanning stage for spatially-resolved measurements.

The samples were prepared by spraying a thin film of nanotube soot about 10 micrometers thick onto copper and sapphire substrates. Note that the film of nanotube soot has a nonuniform thickness and contains contaminants including metal catalyst particles and non-nanotube carbon. For each sample, Q and Δf were measured as a function of probe height from one millimeter down to 100 nanometers. Bare copper and sapphire samples were also measured for comparison.

Results and Discussion

The results of the measurements are shown in Figure 5. We choose to plot the data in the form shown in Figure 5 as it provides a clear visual distinction between bulk metals and bulk dielectrics. By use of a simple model to fit the data for the nanotube-coated copper [8], the conductivity was determined to be 1.9 ± 1.0 X 10^7 S/m. Note that the determined conductivity includes contributions from the underlying copper as well as contaminants in the film. Also note that Δf is always negative due to dominant capacitive coupling with the sample.

At probe heights greater than a few micrometers, the nanotube-coated samples behave in a manner similar to the bulk copper. This is particularly interesting in the case of the sapphire substrate as coating it with nanotube-soot makes it appear similar to bulk copper. Below a few micrometers, the nanotube-coated samples diverge from the bulk copper and from one another. The divergence of the CNT-coated samples from one another shows that this technique is sensitive to the substrate material. This is not surprising as at 2.6 GHz, the evanescent waves penetrate through the 10-μm film and into the substrate. This sensitivity on the material properties of the substrate suggests a role for NSMM as a subsurface probing technique.

The inset to Figure 5 shows a conductivity image of the nanotube film on copper acquired with the NSMM. Contrast in this image arises from differences in conductivity convolved with topography. The image shows a dark spot about 100 μm in diameter at the lower edge of the image that is attributed to a region of low conductivity. This image illustrates the capability for spatially resolved measurements with NSMM.

SUMMARY

We have described two metrological tools for measuring the electromagnetic properties of nanoscale objects in the high-frequency regime. Standard two-port measurement and calibration techniques were used to measure the amplitude and phase of the response of a MWNT up to 24 GHz. NSMM was used to determine the conductivity of thin films at 2.66 GHz and to produce a two-dimensional image of the conductivity. These two tools are part of a new, emerging metrology suite that will be necessary as the electronic and storage industries push the spatial and temporal limits of devices.

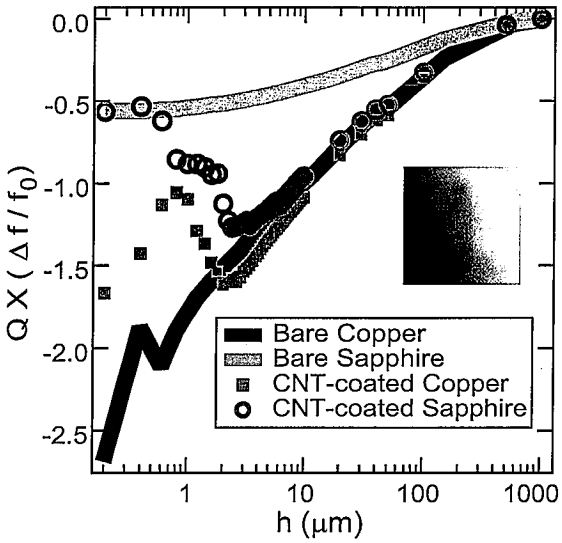

FIGURE 5. The resonator quality factor times normalized frequency shift as a function of probe height for bare copper (solid black line), bare sapphire (solid gray line), carbon nanotube (CNT) -coated copper (gray squares), and CNT-coated sapphire (gray circles). Here, f_0 is the resonator frequency when the sample is absent. The inset on the right is a 1 mm square conductivity image of the CNT-coated sample with the grayscale ranging from low (black) to high (white).

ACKNOWLEDGMENTS

We thank Professor E. Gruelky of the University of Kentucky for the MWNTs. We also thank Dr. J. Lehman for preparation of the samples coated with nanotube soot.

REFERENCES

1. S. Rosenblatt, H. Lin, V. Sazonova, S. Tiwari, and P. L. McEuen, *App. Phys. Letters*, **87**, 153111 (2005).
2. A. A. Pesetski, J. E. Baumgardner, E. Folk, J. X. Przybysz, J. D. Adam, and H. Zhang, *App. Phys. Letters*, **88**, 113103 (2006).
3. D. V. Singh, K. A. Jenkins, J. Appenzeller, D. Neumayer, A. Grill, and H.-S. P. Wong, *IEEE Trans. On Nanotechnology*, **3**, 383 (2004).
4. Z. Yu and P. J. Burke, *Nano Letters*, **5**, 1403 (2005).
5. K. S. Yngvesson, *Appl. Phys. Letters*, **87**, 043503 (2005).
6. M. Zhang, X. Huo, P. C. H. Chan, Q. Liang, Z. K. Tang *Appl. Phys. Letters*, **88**, 163109 (2006).
7. J.-M. Bethoux, H. Happy, G. Dambrine, V. Derycke, M. Goffman, and J.-P. Bourgoin *IEEE Electron. Device Lett.*, **8**, 681 (2006).
8. C. Gao and X.-D. Xiang, *Rev. Sci. Instrum.*, **69**, 3846 (1998).
9. B. T. Rosner and D. van der Weide, *Rev. Sci. Instrum.*, **73**, 2505 (2002).
10. A. Imtiaz, M. Pollak, S. M. Anglage, J. D. Barry, and J. Melngailis, *J. Appl. Phys.*, **97**, 044302 (2005).
11. V. V. Talanov, A. Scherz, R. L. Moreland, and A. R. Schwartz, *Appl. Phys. Letters*, **88**, 134106 (2006).
12. R. B. Marks, *IEEE Trans. Microwave Theory and Techniques*, **39**, 1205 (1991).
13. W. Ding, D. A. Dikin, X. Chen, R. D. Piner, R. S. Ruoff, E. Zussman, X. Wang, and X. Li, *J. Appl. Phys.*, **98**, 014905 (2005).
14. D. M. Pozar, *Microwave Engineering*, Reading, MA: Addison-Wesley, 2003, p. 205.
15. D. F. Williams, C. M. Wang, and U. Arz, *2003 International Microwave Symposium Digest*, 1819 (2003).